Chapter 5

A Landau Theory of the Ripple Phase: Asymmetric ripples in Achiral Membranes

5.1 Introduction

As discussed in earlier chapters, recent freeze fracture and x-ray experiments have shown that the height modulated bilayers in the $P_{\beta'}$ (ripple) [1, 2, 3, 4] phase of phospholipids lack a plane of reflection normal to the ripple wave-vector and hence are asymmetric [5, 6]. On cooling the sample from the L_α phase, metastable symmetric ripples are sometimes seen [7, 8, 9, 10]. These metastable ripples have a wavelength about twice that of the stable asymmetric ripples. The shape of these symmetric ripples has not yet been determined unambiguously. Hentschel and Rustichelli [11] have reported yet another kind of ripple where the height modulation is symmetric but the wavelength is comparable to that of the asymmetric stable ripple phase.

In this chapter we first describe the various theories that have been proposed for the ripple phase. In section-5.2 we discuss the Lubensky-MacKintosh [12, 13] model in detail. In section-5.3 we discuss theories that predict asymmetric modulations in achiral systems. In section-5.4 we discuss our extension of Lubensky-MacKintosh theory which, in contrast to the results of the Lubensky-MacKintosh model, admits the experimentally observed *asymmetric* ripple phase in *achiral* bilayers.

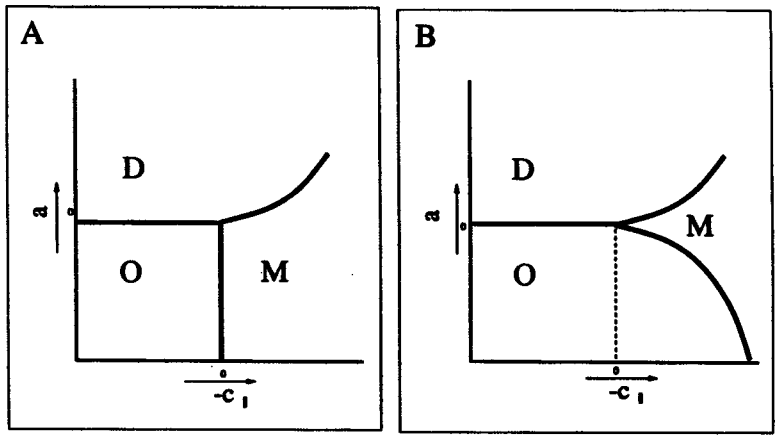

Figure 5.1: Schematic phase-diagrams for the Lifshitz free energy density (eq.:5.1). (**A**) for a vector order parameter and (**B**) for a scalar order parameter. D: disordered phase,O: ordered phase and M: modulated phase.

Before describing the various theories of the ripple phase, it would be relevant to discuss the Landau theory with a Lifshitz point used to describe modulated phases in general.

5.1.1 Lifshitz free energy for modulated phases

Modulated phases can usually be described by a Lifshitz free energy density of the form [14]:

$$f_{Lif} = \frac{1}{2}a\phi^2 + \frac{1}{4}b\phi^4 + \frac{1}{2}c_{\|}(\nabla_{\|}\phi)^2 + \frac{1}{2}c_{\perp}(\nabla_{\perp}\phi)^2 + \frac{1}{2}\alpha(\nabla^2\phi)^2 \qquad (5.1)$$

The field ϕ can be a scalar or a n-component vector. When a, $c_{\|}$ and $c_{\perp}$ are positive, a disordered phase ($\phi = 0$) is the lowest energy state. As a changes sign, the system goes over to an ordered state ($\phi \neq 0$). When both $c_{\|}$ and $c_{\perp}$ are positive, the ordered phase is spatially uniform. If, however, $c_{\|}$ (or $c_{\perp}$) is negative, the system can lower its energy by creating spatially modulated structures with wave-vectors of magnitude $|c_{\|}|/2\alpha$ (or $|c_{\perp}|/2\alpha$). The last term in eq.-5.1 is the stabilizing term and therefore the coefficient α has to be always positive. The phase boundaries between the disordered phase and the two ordered phases are second order lines. The phase boundary between the ordered uniform and the ordered modulated phase is second order when the order parameter is a vector and is first order when the order parameter is a scalar. The three phase boundary lines (separating the ordered phase,

the disordered phase and the modulated phase from each other) meet at the point $a = 0, c_{\|} = 0$ (or $a = 0, c_{\perp} = 0$). This point is called the Lifshitz point (see figure-5.1). The ripple phase, being a modulated phase should also be describable in terms of a Lifshitz like free energy.

5.1.2 Previous theories of the Ripple phase

The theories proposed for the ripple phase fall into two main categories (see appendix A in [15] for a review). (1) Microscopic theories which are based on properties of individual molecules forming the bilayer. (2) Continuum theories in which the bilayers are treated as a continuous membrane. The Landau theories of the ripple phase fall in this category. There are a few other approaches, for example those based on interactions between adjacent bilayers.

Before discussing the theories of the ripple phase, we shall briefly describe the models that have been proposed, based on experimental work, for the structure of this phase. The first model was that of Tardieu et. al. [3] (also see chapter-I). In the Tardieu model the chains of the lipid molecules are assumed to be stiff and parallel. The height modulation of the bilayer is produced by relative sliding movements of the stiff close-packed chains. Helfrich [16] proposed spontaneous curvature as the specific mechanism which may lower the total elastic energy of the rippled bilayers.

Larsson [17] proposed a structure consisting of alternating regions of vertical and tilted chains, for this reason the bilayer is saw-tooth shaped ('folded' in the language used by Larsson). The mechanism proposed by Larsson for the formation of such a structure was the following. It has been experimentally seen [4] that as the sample is heated from the $L_{\beta'}$ phase, at the pre-transition (ie. the $L_{\beta'}$ to $P_{\beta'}$ transition), the chain packing goes from orthorhombic to hexagonal, indicating an increase in the effective chain area (and hence an increase in intra-chain disorder). This would force a simultaneous increase in the head-group area. Larsson postulated that only

a portion of the total chain population becomes disordered at the pre-transition. In that case, a change in the head-group area can be avoided by having alternate regions of tilted and untilted chains. The tilted chains are less disordered and are taken to be in the all-*trans* conformation. The tilt is due to a vertical shift by one zig-zag unit (corresponding to two carbons on the chain) of adjacent chains. The tilted molecules sit in the short arm of the saw-tooth. The disordered chains have a larger cross-sectional area and therefore need not tilt in order to accommodate the head-groups. The untilted chains sit in the long arm of the saw-tooth.

Based on their freeze fracture experiments, Sackmann et. al. [8, 9] proposed a possible structure for both the stable asymmetric and the metastable symmetric ripples. The structure of the stable asymmetric phase is somewhat similar to that proposed by Larsson. The metastable symmetric phase is pictured as being formed by joining a one-wavelength long piece of the ripple with its own mirror image, thus giving the resultant ripples a "M" shape. Here, the driving mechanism of ripple formation is a mismatch between the requirements of the packing of the rigid zig-zag chains and the packing of the head-groups. The difference between this picture and that of Larsson is that here the long and the short arms of the saw-tooth have chains tilted at 28^o (shift by 2 carbon atoms) and 46^o (shift by 4 carbon atoms) instead of 0^o (no shift) and 28^o (shift by 2 carbon atoms) respectively.

Recently Sun et. al. [5], based on their electron density map for the ripple phase obtained from data of ref. [18], have proposed a model where the ripple has a saw-tooth shape; the smaller arm of the saw-tooth has molten L_α like chains and the longer arm has stretched $L_{\beta'}$ like chains. The drawbacks of this model were discussed in chapter-III.

We have reanalyzed the data of ref.- [18] and have shown that all the features of the electron density maps can be explained in terms of a mean tilt of the chains in the

rippling direction (see chapter-II). In our model, the chains are predominantly all-*trans* and parallel to each other. Like in the Tardieu model, the height modulation arises from relative shifting of the chains. In the shorter arm, they make an angle of about 30^o with respect to the local layer normal whereas they are almost parallel to the local layer normal in the longer arm. Thus the shorter arm has a $L_{\beta'}$ like structure and the longer arm has a L_{β} like structure (see chapter-I). Thus our results are in agreement with the model proposed by Larsson.

We now describe the various theories that have been proposed for the ripple phase and discuss their relative merits with reference to the above mentioned structure of $P_{\beta'}$ phase that we have inferred from the electron density maps.

Microscopic theories:

Based on the idea that the inter-chain interactions drive the formation of the ripple phase, Hawthorn and Keeler [19] numerically calculated the van der Waals energy of a spatially modulating layer and showed that in one regime the free energy is lower than that of a flat layer.

In many of the microscopic theories, the packing constraint imposed by the head-groups is an important feature. Pearce and Scott [20] studied a model based on the microscopic mechanism of the competition between the van der Waals attraction between the hydrocarbon chains and the packing hindrance imposed by the head groups. In their description, interactions between the nearest and the next nearest neighbor is taken into account. The Hamiltonian of this system can be reduced to that of the nearest neighbor Ising model (ANNI) under certain approximations. This model exhibits a rippled phase between a high temperature disordered phase and a low temperature ordered phase.

Carlson and Sethna [15] proposed a model where the height modulation of the

bilayer arises due to periodic defect walls. In this model, each lipid molecule is pictured as a head-group attached to a single chain (which represents the average of the two chains). The local packing properties of a one dimensional monolayer of such molecules are described in terms of pair interactions between nearest neighbors. The optimal separation h between the head-groups is taken to be larger than the equilibrium separation r_0 between two free chains. This competition leads to three distinct phases that correspond to a L_α like phase with zero tilt, a uniformly tilted $L_{\beta'}$ like phase and a modulated $P_{\beta'}$ like phase. The minimum energy configuration depends on the size mismatch and the relative strengths of the chain and head group pair interactions.

The van der Waals interaction between neighboring chains is described in terms of a potential $U(r)$, where r is the distance between adjacent chains. $U(r)$ has a minimum at $r = r_0$. The most important feature of $U(r)$ is that it should be soft. As long as $U(r)$ is soft enough, the specific shape of $U(r)$ is not important.

The coupling between the head-groups and the chains is a function of the chain tilt θ alone and is taken to be a harmonic potential: $\frac{1}{2}Wsin^2(\theta)$. r and θ are related by $r = hcos(\theta)$. The free energy, $U(\bar{r}) + \frac{1}{2}Wsin^2(\bar{\theta})$ ($\bar{r}$ and $\bar{\theta}$ are the course-grained versions of the molecular variables r and θ) has three distinct solutions. (1) When $U(r)$ has one global minimum at $\bar{\theta} = 0$, $\bar{r} = h$ and this corresponds to a high temperature, non-tilted L_α like phase. (2) When $U(r)$ has a pair of global minima at $\bar{\theta} = \pm\theta_1$, a uniformly tilted phase like the $L_{\beta'}$ phase is obtained. (3) Solutions corresponding to a modulated $P_{\beta'}$ like phase is also possible. To see this, the zero-force equation for the n^{th} molecule is numerically solved to get the tilt θ_n of the n^{th} molecule. U(r) is taken to be a soft Lennard-Jones potential given by $U(r)=G[(\frac{r_0}{r})^{12} - 2(\frac{r_0}{r})^6]$. The softness of the potential U(r) allows for a solution where the tilt slowly oscillates in space about a zero mean and then suddenly changes direction and then starts to oscillate slowly again, thus giving rise to periodic defect walls. Carlson and Sethna argue that

such walls would result in a height modulation of the bilayers. These three phases are found in the parametric space spanned by $\frac{W}{G}$ and $\frac{h}{r_0}$. They also present a continuum version of their model, which essentially leads to similar results. In this model, the tilt is constrained to be in the ripple direction; but this need not be the case. Also, this model predicts a periodic array of defects in a flat bilayer. It is conjectured that such an array would give rise to a height modulation but the specific mechanism for this is not clear.

Recently, Misbah et. al. [21] have proposed a theory based on electrostatic considerations. This theory is based on the interaction between two sheets of dipoles (head-groups). In this model, a membrane modulation reduces the dipolar energy. At a critical intermembrane distance, the ripple-wave vector goes from zero to a non-zero value. This model is able to account for the experimentally observed asymmetric ripples, which lack a plane of reflection normal to the rippling direction. The main drawback of this theory is that it does not take care of the fact that tilt of the chains is essential for the formation of the ripple phase.

Landau theories of the ripple phase:

Almost all the phenomenological theories of the ripple phase [12, 13, 22, 23, 24, 25, 26] use free energies similar to eq.-5.1, but with different order parameters. Goldstein and Leibler [23] considered a one dimensional modulation of a scalar order parameter given by the bilayer thickness. Using a Lifshitz free energy similar to eq.-5.1, they were able to obtain a modulated structure with a periodic modulation in the bilayer thickness. But from x-ray diffraction data it is clear that the ripple is a periodic height modulation rather than a thickness modulation [4].

Falkovitz et. al. [24] postulate that chain melting is the driving force behind the transition to the ripple phase. In the Falkovitz model as well as in another model proposed by Marder et. al. [25], the order parameter is the bilayer thickness; the

free energy expression has a term favoring either rigid or molten chains, a term proportional to the square of the curvature and a coupling term. These models yield a structure where roughly half of the hydrocarbon chains are melted in the modulated phase. This is inconsistent with the fact that experimentally, the latent heat of the pre-transition is roughly one-tenth of that of the main-transition (the $P_{\beta'}$ to L_α transition), suggesting that only a few of the chains are molten (or disordered) in the ripple phase.

Empirically, the rippling occurs only in those lipids where the chains have a tilt in the lower temperature gel phase. Therefore many theories propose a periodic variation in the chain tilt to explain the rippling. The theory of Doniach [26] again considers a one dimensional modulation in a scalar order parameter now given by the angle between the layer normal and the long axis of the chains. The free energy again has a form similar to eq.-5.1 but the stabilizing term is $(\nabla\phi)^4$ instead of $(\nabla^2\phi)^2$. There is a competition between a preferred tilt and a preferred bilayer curvature and this leads to a modulated structure. This theory predicts the existence of two different kinds of ripples one of which is symmetric and the other asymmetric, depending on the values of the Landau coefficients. In this paper the conditions for the appearance of these two types of ripples is discussed but the phase diagram is not calculated. The main draw back of this theory is that the order parameter is taken to be a scalar given by the magnitude of the tilt, whereas in reality, the direction of the tilt can also vary.

Of all the phenomenological theories proposed so far, the Landau theory of Chen, Lubensky and MacKintosh [12, 13] is probably the most appealing. Here the order parameter is a vector, given by the projection of the chains on the layer plane. Again a Lifshitz free energy similar to eq.-5.1 is used. In this theory, as in many of the earlier theories, the inter bilayer interactions are ignored. This is justified because ripples have been observed in unilamellar vesicles [27]. For achiral systems, this theory predicts the existence of two ripple phases both of which are symmetric. They also

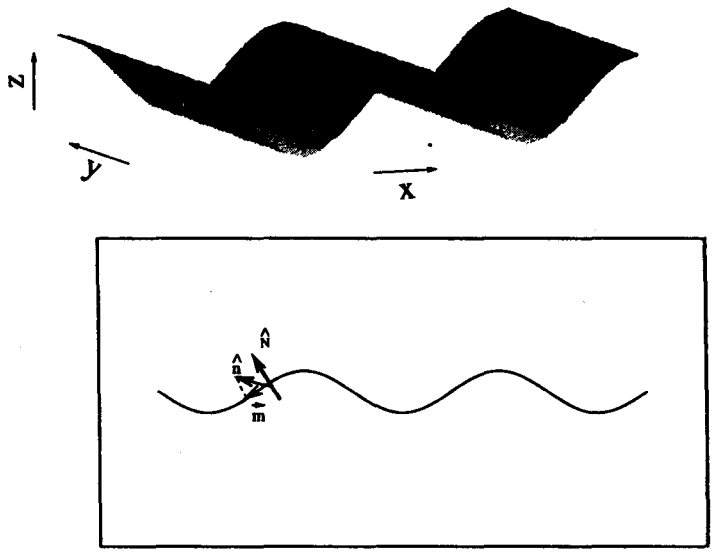

Figure 5.2: Schematic diagram of a rippled bilayer

predict a two dimensionally modulated square lattice phase. According to this theory, asymmetric ripples are allowed only in chiral systems. Thus this theory fails to explain the experimental observation of asymmetric ripples in racemic mixtures [6, 28].

Seifert et. al. [22] have proposed a Landau theory where the order parameter is (as in Lubensky-MacKintosh theory), the projection of the hydrocarbon chains onto the layer plane but here the tilt of the chains in the two leaves of the bilayer need not be coupled. In this model, though the free energy does not explicitly have any chiral terms, the ripple profile can still be asymmetric. The major drawback of this theory is that the predicted shape for the ripple profile is an arc of a circle which is very different from what is seen experimentally.

5.2 The Chen-Lubensky-MacKintosh theory

In this theory [12, 13], the projection of the chains onto a plane tangential to the surface of the bilayer is the vector order parameter (see figure-5.2) and is denoted by **m**.

The Landau-Ginzberg free energy per unit area of the bilayer is:

$$f_{LM} = \frac{1}{2}a|\ \mathbf{m}\ |^2 + \frac{1}{4}b|\ \mathbf{m}\ |^4 + \frac{1}{2}\tilde{c}_{||}(\nabla \cdot \mathbf{m})^2 + \frac{1}{2}c_{\perp}(\nabla \times \mathbf{m})^2 + \frac{1}{2}\alpha(\nabla^2\mathbf{m})^2 \qquad (5.2)$$

The first two terms are the usual Landau terms; the next two terms are the splay and the bend elastic terms; the last term is required for stability, in case one of the two elastic terms becomes negative.

This is the free energy density for the variations in $\mathbf{m}$ on a flat membrane. In a real membrane, the variations in the tilt can couple to the height variable. Therefore, the curvature energy terms:

$$f_c = \frac{1}{2}\kappa(\nabla^2 h)^2 - \gamma(\nabla^2 h)(\nabla \cdot \mathbf{m})$$

have to be added to eq.-5.2. Here 'h' is the height variable in Monge gauge (height measured with respect to the $x-y$ plane), κ is the bending rigidity and γ determines the strength of coupling between the curvature and the gradients in the tilt. A minimization with respect to the height variable 'h' gives the following expression for the height profile that determines the equilibrium membrane shape

$$\nabla^2 h = \frac{\gamma}{\kappa}(\nabla \cdot \mathbf{m}) \qquad (5.3)$$

Using eq.-5.3, the variable h can be eliminated from the total free energy density. This leads to the same expression for the free energy density as eq.-5.2 but with the coefficient of the splay term renormalized to : $(c_{||} = \tilde{c}_{||} - \gamma^2/\kappa)$. thus the effective free energy density reads:

$$f_{LM} = \frac{1}{2}a|\ \mathbf{m}\ |^2 + \frac{1}{4}b|\ \mathbf{m}\ |^4 + \frac{1}{2}c_{||}(\nabla \cdot \mathbf{m})^2 + \frac{1}{2}c_{\perp}(\nabla \times \mathbf{m})^2 + \frac{1}{2}\alpha(\nabla^2\mathbf{m})^2 \qquad (5.4)$$

If this renormalized splay elastic coefficient $c_{||}$ becomes negative, the bilayers have a spontaneous local curvature and can have periodic modulations. To determine the mean-field phase diagram, a single wave length modulation is assumed. Under this assumption, all the possible ripple phases can be described by the ansatz:

$$m_x = m_0^L + m_1^L cos(qx)$$

$$m_y = m_0^T + m_1^T sin(qx)$$

The modulation is assumed to be in the x-direction. It can be shown that a phase with $m_0^L \neq 0$ is not possible. Thus in this theory, there cannot be an average tilt in a direction parallel to the modulation direction. Three distinct ripple phases are possible, depending on which of the coefficients m_1^L, m_0^T and m_1^T are non-zero.

- when $m_1^L \neq 0$, $m_0^T \neq 0$ and $m_1^T = 0$, the ripple is symmetric and the phase is called $P_{\beta'}^{(1)}$ phase.
- when $m_1^L \neq 0$, $m_0^T = 0$ and $m_1^T = 0$, the ripple is still symmetric and the phase is called $P_{\beta'}^{(2)}$ phase.
- when $m_1^L \neq 0$, $m_0^T = 0$ and $m_1^T \neq 0$, the ripple is again symmetric but the winding number is one and not zero like in the other two phases described above. This phase is called $P_{\beta'}^{(3)}$ phase.

These phases differ from each other in having different spatial variation of $\mathbf{m}$ (see [12, 13] for a pictorial representation). Apart from these, a square lattice phase described by

$$m_x = m_1 cos(qx)$$

$$m_y = m_1 cos(qy)$$

is also considered. The free energy density of the various phases described above is calculated and then integrated over one wavelength to get the average free energy density. The average free energy density is then minimized with respect to the amplitudes of the components of $\mathbf{m}$ and the wave-vector q to get the equilibrium values of these coefficients in terms of the Landau parameters. These values are put back into the free energy expression and the free energy for the various phases are equated to determine the phase boundaries. A schematic phase diagram for this model is shown in figure-5.3

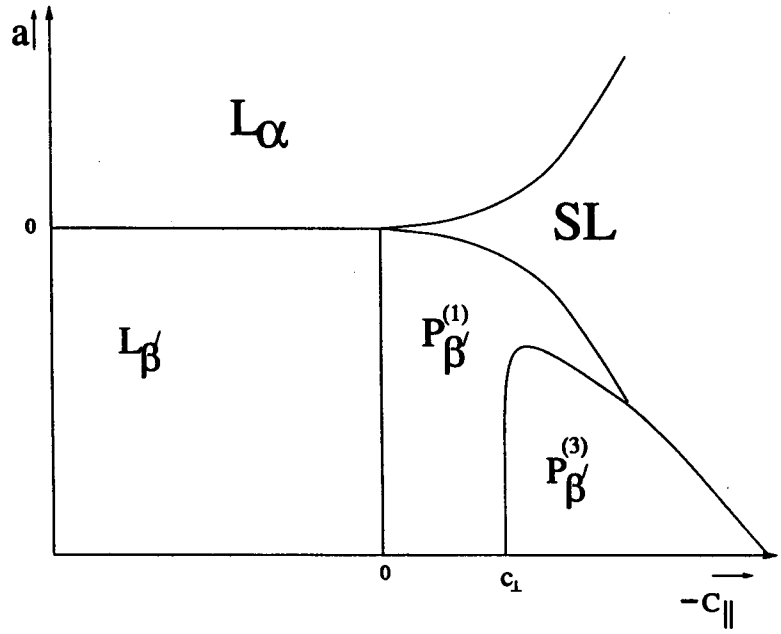

Figure 5.3: A schematic phase-diagram for the Landau-MacKintosh model for achiral membranes. SL: square lattice phase, $P_{\beta'}^{(1)}$ and $P_{\beta'}^{(3)}$ are modulated phases where the modulations is symmetric. See [12, 13] for details.

If the system is chiral, the free energy can have additional symmetry allowed terms. The lowest order chiral term is $\lambda_b \mid \mathbf{m} \mid^2 (\nabla \times \mathbf{m})$. Apart from this the chiral coupling of the tilt to the membrane shape, $\lambda_{HP}\epsilon_{ki}(\nabla_i\nabla_j h)m_j m_k$ also has to be added. This is the Helfrich-Prost [29] term that accounts for the tendency of the molecules of a chiral two-dimensional membrane embedded in a three dimensional space to twist. As in the achiral case, the effective free energy in terms of the tilt $\mathbf{m}$ can be found by a functional minimization of the free energy with respect to h. This gives:

$$\begin{aligned} f_{LM} &= \frac{1}{2}a\mid \mathbf{m} \mid^2 + \frac{1}{4}b\mid \mathbf{m} \mid^4 + \frac{1}{2}c_\parallel(\nabla\cdot\mathbf{m})^2 + \frac{1}{2}c_\perp(\nabla\times\mathbf{m})^2 + \frac{1}{2}\alpha(\nabla^2\mathbf{m})^2 + \\ &\quad \lambda_b' \mid \mathbf{m} \mid^2 (\nabla\times\mathbf{m}) \end{aligned} \tag{5.5}$$

here

$$\lambda_b' = \lambda_b + \frac{\lambda_{HP}}{2\kappa}$$

The height is now given by

$$\nabla^4 h = \frac{\gamma}{\kappa}\nabla^2(\nabla\cdot\mathbf{m}) - \frac{\lambda_{HP}}{\kappa}\epsilon_{ki}[\nabla_i\nabla_j(m_j)(m_k)]$$

the resulting profiles can be expressed as a Fourier series:

$$h(x) = a_1 sin(qx) + a_2 sin(2qx) + b_2 cos(2qx) + a_3 sin(3qx) + b_3 cos(3qx) + ... \tag{5.6}$$

It can be shown that in the $P_{\beta'}^3$ phase both a_1 and a_2 are non-zero thus giving an asymmetric height profile. Thus in the Lubensky-MacKintosh theory, an asymmetric ripple profile is expected only for chiral systems. Therefore, a clear prediction of this model is the existence of only symmetric ripples in an achiral system.

To test this prediction, Katsaras and Raghunathan looked at the x-ray diffraction from racemic mixture (achiral) of DMPC and found that the ripples were asymmetric [28]. This result could still have been accounted for by this theory if the two enantiomers in the racemic mixture had separated and formed chiral domains within the bilayer. This possibility has been ruled out by later experiments [30]. It is therefore clear that some modification to the Lubensky-MacKintosh theory is required to account for the occurrence of asymmetric ripples in achiral systems.

5.3 Previous theories that predict asymmetric modulations in achiral systems

5.3.1 Doniach's theory:

In Doniac's theory [26] a competition between a preferred layer curvature imposed by the head-group interactions and a preferred tilt imposed by the chain-chain interactions gives rise to the rippled structure. The magnitude of the tilt angle θ is the order parameter. The free energy density is written as:

$$f_{don} = \frac{1}{a}\{\lambda[(\frac{ad\theta}{dx})^2 - {\theta_0}'^2] + \gamma(\theta^2 - {\theta_0}^2)^2\} \tag{5.7}$$

where a is a length scale of the order of inter-chain distance. The first term sets the preferred curvature to θ_0' and the second term sets the preferred tilt to θ_0.

In the language we have been using so far, the above free energy would be of the form:

$$f_{don} = \frac{1}{2}a\theta^2 + \frac{1}{4}b\theta^4 + \frac{1}{2}c(\nabla_x\theta)^2 + \frac{1}{4}\beta(\nabla_x\theta)^4 \tag{5.8}$$

This is similar to eq.5.1 except that the stabilizing term now is $(\nabla_x\theta)^4$ instead of

$(\nabla_x^2\theta)^2$. Also, in eq.-5.8, all the coefficients are not independent of each other.

The bilayer height profile is calculated for different values of the coefficients. Two regimes are identified depending on the value of the dimensionless quantity $\eta = (\frac{\theta_0'}{\theta_0})^2(\frac{\lambda}{3\gamma})^{\frac{1}{2}}$. When $\eta < 1$, the tilt oscillates in space between θ_{max} and θ_{min} but the average remains non-zero. When $\eta > 1$, the tilt oscillates about a zero mean. The tangent of the angle $\theta(x)$ at point x gives the slope of the membrane at x. This is integrated with respect to x to get the height profile $y(x)$. The first case ($\eta < 1$) corresponds to an asymmetric height profile and the second case ($\eta > 1$) to symmetric height profile. The main drawback of this theory is that here the tilt order parameter is a scalar whereas in reality, not only the magnitude but also the direction of the tilt can vary.

5.3.2 The "rippled commensurate phase" of Jacobs et. al.

Jacobs et. al. [31] studied a *one dimensional* model with a real scalar order parameter (ϕ) that depends on a single spatial coordinate and showed that the inclusion of the higher order term $(\nabla_x\phi)^4$ in the free energy density induces a phase where the order parameter oscillates about a non-zero mean value.

The free energy here is:

$$f_{jac} = \frac{1}{2}a\phi^2 + \frac{1}{4}b\phi^4 + \frac{1}{2}c(\nabla_x\phi)^2 + \frac{1}{2}\alpha(\nabla_x^2\phi)^2 + \frac{1}{4}\beta(\nabla_x\phi)^4 \qquad (5.9)$$

where the last term is the new higher order term. Both the $(\nabla_x^2\phi)^2$ term and the $(\nabla_x\phi)^4$ term are stabilizing terms. This reduces to the Lifshitz free energy (eq.5.1) in the $\beta = 0$ limit and the Doniach model (eq.5.8) in the $\alpha = 0$ limit.

For the case $\beta = 0$ in eq.-5.9, the order parameter in the modulated phase has a zero spatial average and can therefore be Fourier expanded as $\phi(x) = \sum_{n=1}^{N} \phi_n sin(2n - 1)qx$. This phase is a symmetrically modulated phase. In the uniformly ordered

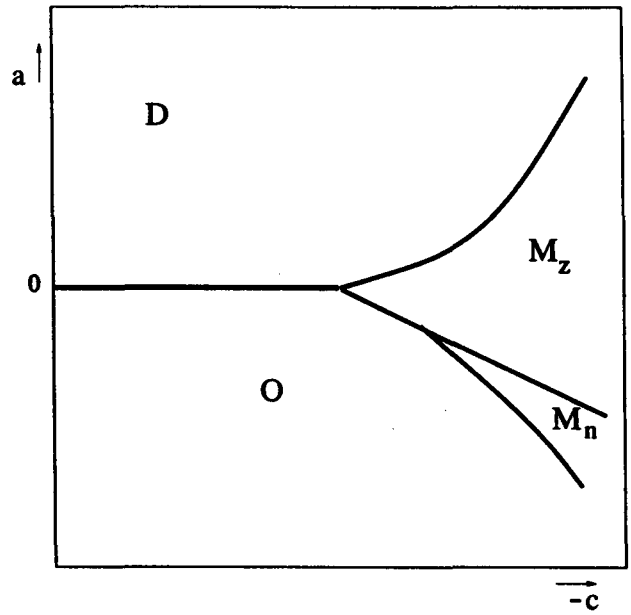

Figure 5.4: A schematic phase diagram for the Jacobs model. D: disordered phase, O: ordered phase, M_z: modulated phase with order parameter oscillations around a zero mean, M_n: modulated phase with order parameter oscillations around a non-zero mean.

phase, (for both $\beta = 0$ and $\beta \neq 0$) the order parameter has a value $\phi = \pm\phi_c \neq 0$. They also show that the ordered phase is unstable to oscillations of ϕ about ϕ_c for $a > \frac{-c^2}{8\alpha}$. However, when $\beta = 0$, this line falls in the region of stability of the symmetrically modulated phase and hence a phase were ϕ oscillates about a non-zero mean is not obtained.

When β is increased from zero, the symmetrically-modulated to uniformly-ordered phase transition line goes up in the $a - c$ plane. Eventually it crosses the $a = -\frac{c^2}{8\alpha}$ line, above which ϕ oscillates about ϕ_c. Hence if β is large enough, there is now a region in the $a - c$ plane, where the order parameter oscillates around a non-zero mean. A schematic phase diagram is given in figure-5.4.

5.3.3 Analytical calculations of Benguigui

Benguigui [32] obtained the $a - c$ phase diagram analytically for the Jacobs model assuming a sinusoidal variation in the order parameter ϕ. He used this model to explain the Smectic-A_R liquid crystalline phase. In this model, the order parameter

is the polarization vector which has both x and z dependence. In the present discussion, for the sake of clarity, we suppress the z dependence: this does not affect the arguments or conclusions.

An ansatz $\phi = \phi_0 + \phi_1 sin(qx)$ is put in eq. 5.9 and the $a - c$ phase diagram is constructed. The possible phases are: Smectic-A_1 (ϕ_0=0,ϕ_1=0), Smectic-A_2 ($\phi_0 \neq$0,ϕ_1=0), Smectic-$\tilde{A}$ (ϕ_0=0,$\phi_1 \neq$0) and Smectic-A_R ($\phi_0 \neq$0,$\phi_1 \neq$0). In case of phase transitions in phospholipid membranes with the order parameter given by the magnitude of the tilt of the hydrocarbon chains, the corresponding phases would be: untilted L_α phase (ϕ_0=0,ϕ_1=0), uniformly tilted $L_{\beta'}$ phase ($\phi_0 \neq$0,ϕ_1=0), symmetric ripple phase with no mean tilt (ϕ_0=0,$\phi_1 \neq$0) and asymmetric ripple phase where the tilt oscillates about a non-zero mean ($\phi_0 \neq$0,$\phi_1 \neq$0). The coordinates of the triple point where the uniformly tilted, symmetrically oscillating and asymmetrically oscillating phases coexist is determined to be [1] :

$$a_{trip} = -\frac{10b\alpha}{4\beta}\ , \quad c_{trip} = -2\alpha\sqrt{\frac{5b}{\beta}}\ . \tag{5.10}$$

These expressions are only approximate since in the derivation, the higher order terms where dropped. The actual coordinates of the triple point on the numerically calculated phase diagram are therefore different (see [31] and figure-5.4 and -5.6), though eq.-5.10 indicates correctly the trend of the dependence of a_{trip} and c_{trip} on the other Landau coefficients.

5.4 A Landau theory for achiral bilayers

We now extend the Chen-Lubensky-MacKintosh model by including the higher order term introduced by Jacobs et. al. and an anisotropy of the bending modulus of the bilayer. With these modifications, we are able to account for asymmetric ripples in achiral bilayers.

[1] There is a minor mistake in the expression in ref. [32] that has been corrected here.

The order parameter here (as in the Lubensky-MacKintosh model [12, 13]) is the projection $\mathbf{m}$ of the chains on to the local tangent plane. One has to deal with a vector order parameter that can be a function of either one or two spatial coordinates. The mean bilayer plane is taken to be the $x-y$ plane and the ripple is taken along the x-direction (see figure-5.2). The bend elastic term $(\nabla \times \mathbf{m})^2$ is not included in this free energy. The inclusion of this term would simply lead to some parts of the phase diagram now occupied by the asymmetric ripple being taken over by a winding phase [12, 13] (with a non-zero $\nabla \times \mathbf{m}$). If the fact that in the ripple phase the chains are packed parallel is taken into account, the winding phase, where the chains are not parallel to one another, is expected to be energetically unfavorable. In this case the free energy density is:

$$f = \frac{1}{2}a|\ \mathbf{m}\ |^2 + \frac{1}{4}b|\ \mathbf{m}\ |^4 + \frac{1}{2}c(\nabla \cdot \mathbf{m})^2 + \frac{1}{2}\alpha(\nabla^2\mathbf{m})^2 + \frac{1}{4}\beta(\nabla \cdot \mathbf{m})^4 \qquad (5.11)$$

Here the coefficient c of the $(\nabla \cdot \mathbf{m})^2$ term is the renormalized (see the discussion of Lubensky-MacKintosh theory) splay coefficient. We assume the following ansatz for $\mathbf{m}$:

$$\begin{aligned} m_x &= m_{0x} + m_{1x}cos(qx) + m_{2x}cos(2qx) \\ m_y &= m_{0y} + m_{1y}cos(qx) \end{aligned} \qquad (5.12)$$

The ripple is always in the x-direction. Depending on the value of the coefficients m_{0x}, m_{1x}, m_{0y} and m_{1y}, various kinds of ripples are obtained. It can be seen from our numerical results that $m_{2x} \neq 0$ if and only if $m_{0x} \neq 0$. Following types of ripple phases are allowed:

- A symmetric ripple phase with no mean tilt: the tilt oscillates sinusoidally about a zero mean. This will be referred to as the P_β phase. This corresponds to $m_{0x} = 0, m_{0y} = 0, m_{1x} \neq 0, m_{1y} = 0,\ m_{2x} = 0$.

- A symmetric ripple phase where the tilt oscillates sinusoidally about a non-zero tilt in a direction perpendicular to the ripple direction. This will be referred to

as the $P^t_{\beta'}$ phase (this is same as $P^{(1)}_{\beta'}$ phase in [12, 13]). This corresponds to $m_{0x} = 0, m_{0y} \neq 0, m_{1x} \neq 0, m_{1y} = 0, m_{2x} = 0$.

- An asymmetric ripple phase where the chains oscillate about a non-zero mean tilt in the ripple direction. We have checked that in this case the modulation is unstable with respect to a second harmonic and hence this implies an asymmetric ripple profile (ie. $m_{2x} \neq 0$). This phase will be referred to as the $P^l_{\beta'}$ phase. This corresponds to $m_{0x} \neq 0, m_{0y} = 0, m_{1x} \neq 0, m_{1y} = 0, m_{2x} \neq 0$.

- A square lattice phase characterized by a 2-dimensional ripple. This is same as the square lattice phase in the Chen-Lubensky-MacKintosh model. This is called the $P^{2D}_{\beta'}$ phase. Here the ansatz for $\mathbf{m}$ is

$$m_x = m_1 cos(qx)$$

$$m_y = m_1 cos(qy)$$

The L_α phase is characterized by $m_{0x} = 0, m_{0y} = 0, m_{1x} = 0, m_{1y} = 0, m_{2x} = 0$ and the $L_{\beta'}$ phase by $m_{0x} \neq 0, m_{0y} = 0, m_{1x} = 0, m_{1y} = 0, m_{2x} = 0$.

The phase transitions from the flat phases and also between the various kinds of ripples take place as the values of a and c are varied and hence the $a - c$ phase diagram is plotted here. In case of a vector order parameter $\mathbf{m}$, it is not possible to calculate the phase boundaries analytically as was done in reference [32] since with this free energy expression, it would involve solving cubic equations. Therefore, the phase diagrams presented here are numerically calculated.

The following procedure is adopted to calculate the phase diagrams. The ansatz for $\mathbf{m}$ corresponding to one of the ripple profiles described above is put in eq.-5.11 and the free energy density is integrated over a wavelength and then divided by the wavelength to obtain the average free energy density. The free energy density is then numerically minimized [2] with respect the wave-number q and the coefficients of the

[2] The simplex method (amoeba) described in ref. [33] is used to do the minimization

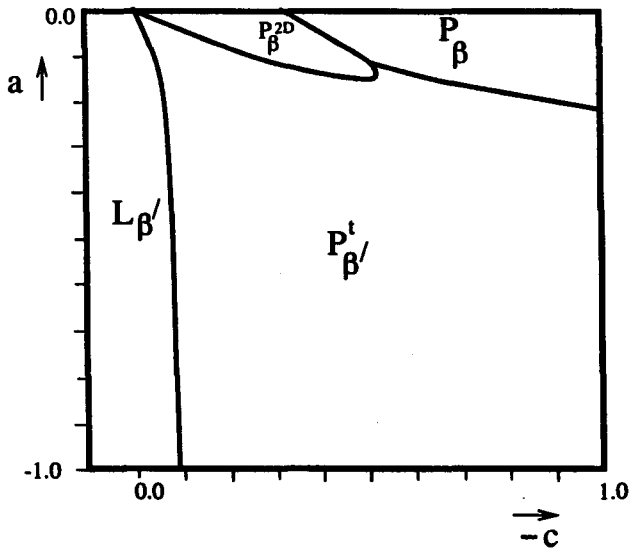

Figure 5.5: The phase diagram for a 2-dimensional system with free energy given by equation 5.11. Here b=1.0, α=1.0 and β=4.00

components of **m**: $m0_x, m1_x, m0_y, m1_y$ etc. This is done for fixed values of the coefficients b, α, β, a and c. a and c are varied over a range and the above procedure is repeated. This gives the value of the free energy for a particular kind of ripple, at each value of a and c. This is done for all the different ripples described above. The energy for each kind of ripple is then compared and the minimum energy configuration at each point on the a-c plane is identified.

When the tilt is restricted to be in the direction of the ripple, ie. in the *one dimensional limit* (same as [31]), the asymmetric $P^l_{\beta'}$ phase is obtained in parts of the $a-c$ plane and the results of ref. [31] are recovered. When this constraint is removed and **m** is allowed to have a component perpendicular to the ripple, ie. in the *two dimensional* case, the $P^l_{\beta'}$ phase goes over to the $P^t_{\beta'}$ phase. In other words, it costs less energy to have spatial tilt oscillations in a direction perpendicular to the direction of average tilt. Therefore in the two dimensional case, m_{0x} is always equal to zero in the modulated phase. This case is similar to the case discussed in ref.- [12], except that the term $(\nabla.\mathbf{m})^4$ destabilizes the two dimensional square lattice phase in favor of the one-dimensional symmetric ripple with no mean tilt (figure-5.5).

From the above discussion we conclude that if due to some reason the tilt is constrained to be in the rippling direction, an asymmetric ripple is possible even in an achiral systems. An anisotropy in the elastic constants is a mechanism by which the tilt can be constrained. In a layered system where the molecules are tilted with respect to the layer normal, a curvature in the direction of the tilt and a curvature orthogonal to the tilt may have different energies. In thermotropic systems, it has been shown that near the Smectic-A to Smectic-C transition, a curvature of the layer transverse to the direction of $\mathbf{m}$ is energetically more favorable than a tilt in the direction of curvature [34]. But deep inside the Smectic-C phase, this need not necessarily be true. In the case of lipid bilayers, the L_α phase is the analogue of the Smectic-A phase and the $L_{\beta'}$ phase is the analogue of the Smectic-C phase. We are interested in transitions from a tilted phase ($L_{\beta'}$) to a modulated phase. Therefore the anisotropy in the elastic constants here need not necessarily favor a transverse tilt. In fact, if the one constant approximation imposed in ref. [34] is lifted and higher order terms are included, it can be shown that under certain conditions, a bilayer curvature in the direction of the tilt is favored [35].

5.4.1 The anisotropy in the elastic constant

In a system where the molecules are tilted, symmetry considerations allow the elasticity of the $\mathbf{m}$- field to be anisotropic. Therefore the anisotropy terms given by

$$\frac{\xi}{2}[(\mathbf{m}\cdot\nabla)\mathbf{m}]^2+\frac{\zeta}{2}[(\mathbf{m}\times\nabla)\mathbf{m}]^2$$

are added to eq.-5.11. When there is a nonzero mean tilt, these terms distinguish between gradients of $\mathbf{m}$ along $\mathbf{m}$ and gradients of $\mathbf{m}$ orthogonal to $\mathbf{m}$.

The full free energy reads:

$$\begin{aligned} f &= \frac{1}{2}a|\,\mathbf{m}\,|^2+\frac{1}{4}b|\,\mathbf{m}\,|^4+\frac{1}{2}c(\nabla\cdot\mathbf{m})^2+\frac{1}{2}\alpha(\nabla^2\mathbf{m})^2+\frac{1}{4}\beta(\nabla\cdot\mathbf{m})^4+ \\ &\quad \frac{\xi}{2}[(\mathbf{m}\cdot\nabla)\mathbf{m}]^2+\frac{\zeta}{2}[(\mathbf{m}\times\nabla)\mathbf{m}]^2 \end{aligned} \tag{5.13}$$

As before, the height profile is related to the tilt via equation 5.3.

The phase diagram

The phase diagram is calculated as before and is shown in figure-5.6 (for $\xi < \zeta$) and in figure-5.7 (for $\xi > \zeta$). When $\xi < \zeta$ it is easier to bend the bilayer in the direction of the tilt. In the region of the parameter space shown, $|\mathbf{m}| \leq 0.5$. We find two major differences from the phase diagram obtained from the Lubensky-MacKintosh model. Firstly, the square lattice phase is not stable in the present model. This is expected since because of the anisotropy in the elastic constants, modulations in one direction is favored over modulations in the other directions. This is consistent with the fact that such a phase has never been experimentally observed. Secondly, the $P^{l}_{\beta'}$ phase is now stable in part of the parameter space. In this phase m_{2x} is always non-zero and hence, as can be seen from eq.-5.3, the ripple profile is asymmetric. However the asymmetry is rather small; m_{2x} is typically two orders of magnitude smaller than m_{1x}. This is about an order of magnitude smaller than that observed experimentally. As discussed before, (eq.-5.10), the coordinates of the $P^{l}_{\beta'}$-$P^{t}_{\beta'}$-$L_{\beta'}$ triple point depend on the ratio α/β of the two stabilizing terms. As this ratio is decreased, the triple point moves towards the origin. Note that $L_{\beta'}$ phase is now stable till $(c_{\|} + \xi m_o^2)$ or $(c_{\|} + \zeta m_o^2)$ becomes negative.

When $\zeta < \xi$, the $P^{l}_{\beta'}$ phase disappears from the phase diagram (figure-5.7). This is similar to the $\xi = \zeta = 0$ case except that the square lattice phase is now absent.

5.4.2 A different ansatz

Experimentally, the ripple profile is usually saw-tooth shaped. It is therefore better approximated by the following ansatz for the height $h(x)$ profile:

$$h(x) = \eta \; tanh(\nu x) - \mu x \tag{5.14}$$

here η and ν are constants to be determined by the minimization of the free energy. μ is related to the wavelength by the fact that the height $h(x)$ has to go to zero at

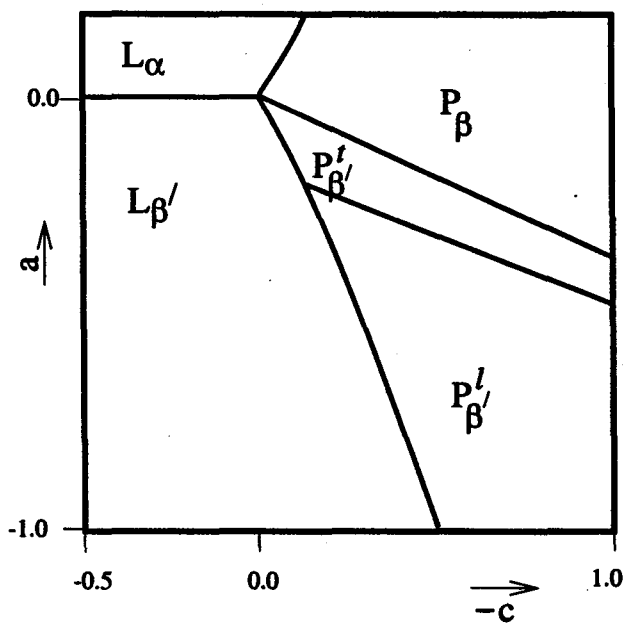

Figure 5.6: Numerically calculated mean-field phase diagram for an achiral membrane, free energy is given by eq.-5.13 with b=1.0, α=0.01, β=4.0, ξ=0.1 and ζ=0.7.

$\pm\pi/q$ where q is the wave-number. Figure-5.8 shows a possible height profile drawn using this ansatz.

The tilt **m** is then given by (see eq.-5.3)

$$m(x) = \eta\ sech^2(\nu x) + \rho x$$

ρ is a constant of integration. This ansatz for **m** is put in eq.-5.13 (ie. the free energy expression), the free energy density is integrated over a wavelength and divided by the wavelength to get the average free energy density and then minimization is done with respect to η, ν, ρ and q.

This ansatz was found to give typically about 20 % lower values of the free energy compared to the Fourier ansatz (eq.-5.12) at all points in the parameter space corresponding to the different ripple phases. The height profile was found to be always weakly asymmetric, consistent with the weak asymmetry seen in the $P^l_{\beta'}$ phase using the Fourier ansatz. In this phase $|\mathbf{m}_o| >> 0$, whereas in the other ripple phases $|\mathbf{m}_o| \approx 0$. Further, in the $P^l_{\beta'}$ phase the longer arm of the asymmetric ripple has a

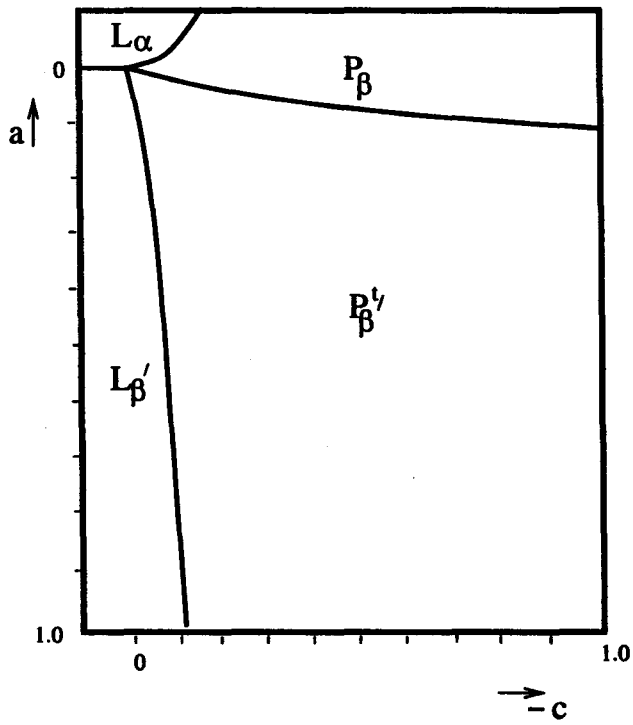

Figure 5.7: Numerically calculated mean-field phase diagram for an achiral membrane, free energy is given by eq.-5.13 with b=1.0, α=0.01, β=4.0, ξ=0.7 and ζ=0.1.

lower value of $\mathbf{m}$. We have checked that the phase diagram obtained with this ansatz is qualitatively similar to that deduced using the Fourier ansatz, though the present ansatz cannot differentiate between the $P^t_{\beta'}$ and P_β phases.

A physical picture

In order to understand the origin of the asymmetric ripples, we first consider the stability to height modulations of a bilayer where the equilibrium mean value of the chain tilt is non zero and is given by $\mathbf{m_o}$. With $\xi < \zeta$ in eq.-5.13, variations in $\mathbf{m}$ along $\mathbf{m_o}$ are favored over those perpendicular to $\mathbf{m_o}$. At sufficiently small values of the coefficient of $(\nabla \cdot \mathbf{m})^2$, the system becomes unstable to the formation of ripples with a wave-vector along $\mathbf{m_o}$ (recall that a non-zero $\nabla \cdot \mathbf{m}$ implies a non-zero curvature in height: eq.-5.3). Let $\mathbf{m} = \mathbf{m_o} + \delta\mathbf{m}$ (where $\delta\mathbf{m}$ is a small variation in $\mathbf{m}$ due to the rippling). The term proportional to $\mid m_o \mid^2 (\mathbf{m_o} \cdot \delta\mathbf{m})$ (coming from the term $\mid \mathbf{m} \mid^4$ in the free energy) ensures that it is favorable to have $\delta\mathbf{m}$ in the direction opposite to $\mathbf{m_o}$. That is, it costs less energy to decrease the tilt than to increase it. Now the system can lower its energy by taking advantage of the symmetry-allowed bias

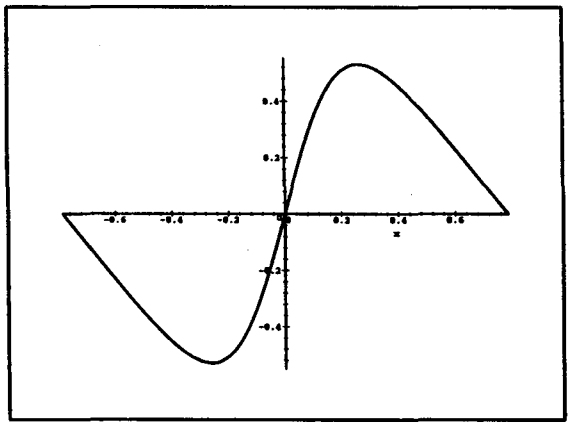

Figure 5.8: A height profile drawn using equation 5.14 for η =0.5, ν =5.0, μ =1.0 and q =4.0.

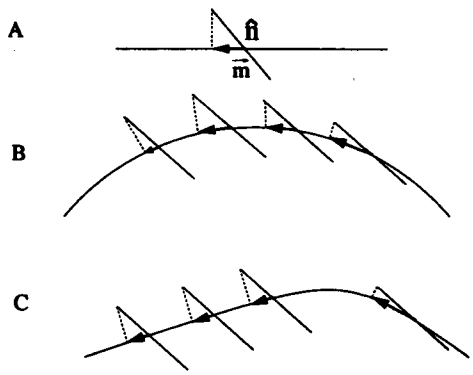

Figure 5.9: a: **m** for a flat bilayer, b: **m** for a bilayer with uniform curvature corresponding to a symmetric ripple profile. Though all the chains make the same angle with respect to the z-axis, the angle with respect to the bilayer normal increases as one goes from left to right. C: The length of left side of the symmetric profile has been increased to maximize the region of favorable tilt.

discussed above. If the ripple shape is asymmetric and in the longer arm of the ripple $\delta \mathbf{m} < 0$, the energy can be lowered. Thus the presence of a mean tilt along the ripple wave-vector favors asymmetric ripples (figure-5.9) with an asymmetric height profile

It is clear from the above discussion that the effective bending modulus of the bilayer must be smaller in the direction of the mean tilt in order to see asymmetric ripples. We may now speculate on the origin of this kind of anisotropy in the bending modulus. It is well known that the tilt of the hydrocarbon chains with respect to the bilayer normal is achieved by relative sliding of the chains along their long axes. If the chains

are constrained to be parallel, as seems to be the case in lipid bilayers, the curvature of the bilayer is produced by gradients in this sliding displacement. Thus the molecular tilt as well as the bilayer curvature result from the same basic molecular mechanism. When the chains are tilted, the overlap between two adjacent chains along the tilting direction decreases, whereas in the perpendicular direction the overlap remains the same as in the untilted phase. Therefore, the net restoring force between the chains can be expected to be lower in the tilt direction, making it easier for the bilayer to bend in this direction.

5.5 Conclusion

In this chapter we have discussed the various theories that have so far been proposed to explain the ripple phase of phospholipids and have explained the drawbacks of each theory. We have extended the Landau theory of Chen-Lubensky-MacKintosh to account for asymmetric ripples in achiral systems. In contrast to the results of the Lubensky-MacKintosh model, our model admits the experimentally observed *asymmetric* ripple phase in *achiral* bilayers. Further, we show that the two- dimensionally modulated square lattice phase predicted by the Lubensky-MacKintosh model is not stable. Our model thus removes some discrepancies between the results of the Lubensky-MacKintosh model and experimental observations.

Bibliography

[1] F. C. MacKintosh, Current Opinion in Colloid and Interface Science **2,** 382 (1997).

[2] G.S. Smith, E.B. Sirota, C.R. Safinya, and N.A. Clark, Phys. Rev. Lett. **60,** 813 (1988).

[3] A. Tardieu, V. Luzzati, and F. C. Reman, J. Mol. Biol. **75,** 711 (1973).

[4] M. J. Janiak, D. M. Small, and G. G. Shipley, J. Biol. Chem. **254,** 6068 (1979).

[5] W.-J. Sun, S. Tristram-Nagle, R. M. Suter, and J. F. Nagle, Proc. Natl. Acad. Sci. USA **93,**.

[6] J. A. Zasadzinski, Biochim. Biophys. Acta **946,** 235 (1988).

[7] H. Yao, S. Matuoka, B. Tenchov, and I. Hatta, Biophys. J. **59,** 252 (1991).

[8] E. Sackmann, D. Ruppel and C. Gebhardt, Liquid Crystals of One - and Two-Dimensional Order, W. Helfrich and G. Heppke (ed.), Springer Series in Chemical Physics 11, Springer-Verlag, 1980.

[9] D. Ruppel and E. Sackmann, J. Phys. (Paris) **44,** 1025 (1983).

[10] J. A. N. Zasadzinski and M. B. Schneider, J. Phys. (Paris) **48,** 2001 (1987).

[11] M.P. Hentschel and F. Rustichelli, Phys. Rev. Lett. **66** 903 (1991).

[12] T. C. Lubensky and F. C. MacKintosh, Phys. Rev. Lett. **71,** 1565 (1993);

[13] C.-M. Chen, T.C. Lubensky, and F.C. MacKintosh, Phys. Rev. E **51,** 504 (1995).

[14] P. M. Chiekin and T. C. Lubensky, Principles of Condensed matter physics. Cambridge University Press, New York, 1995.

[15] J. M. Carlson and J. P. Sethna, Phys. Rev. E **36**, 3359 (1987).

[16] W. Helfric, Z. Naturforsch. **29C**, 692 (1974).

[17] K. Larsson, Chem. Phys. Lipids, **20** 225 (1977).

[18] D. C. Wack and W. W. Webb, Phys. Rev. lett., **61**, 1210 (1988).
D. C. Wack. W. W. Webb, Phys. Rev. A **40**, 2712 (1989).

[19] Hawthorn and Keeler, Phys. Rev. A, **33** 3333 (1986).

[20] P. A. Pearce and H. L. Scott, J. Chem. Phys., **77** 951 (1982).

[21] C. Misbah, J. Duplat and B. Houchmandzahed, Phys. Rev. Lett. **80** 4598 (1998).

[22] U. Seifert, J. Shillcock and P. Nelson, Phys. Rev. Lett. **77**, 5237 (1996).

[23] R. E. Goldstein and S. Leibler, Phys. Rev. Lett. **61**, 2213 (1988)

[24] M. S. Falkovitz, M. Seul, H. L. Frisch and H. M. McConne ll, Proc. Nat. Acad. Sci. U.S.A. **81** 3918 (1982).

[25] M. Marder, H. L. Frisch, J. S. Lagner and H. M. McConnell, Proc. Nat. Acad. Sci. U.S.A. **81**, 6559 (1984).

[26] S. Doniach, J. Chem. Phys. **70** 4587 (1979)

[27] P. C. Mason, B. D. Gaulin, R. M. Epand, G. D. Wignall and J. S. Lin, Phys. Rev. E **59** 3361 (1999)

[28] J. Katsaras and V. A. Raghunathan, Phys. Rev. Lett. **74**, 2022 (1995).

[29] W. Helfrich and J. Prost, Phys. Rev. A **38** 3065 (1988).

[30] J. Katsaras, R. F. Epand, and R. M. Epand, Phys. Rev. E **55**, 3751 (1997).

[31] A. E. Jacobs, C. Grein, and F. Marsiglio, Phys. Rev. B **29**, 4179 (1984).

[32] L. Benguigui Phys. Rev. A **33** 1429 (1986).

[33] W.H. Press, S.A. Teukolsky, W.T.Vellerling, and B.P. Flannery, Numerical Recipes (Cambridge University Press, 1997).

[34] Y. Hatwalne and T. C. Lubensky, Phys. Rev. E, **52** 6240 (1995).

[35] Yashodhan V. Hatwalne, *unpublished result.*